Automatika

Journal for Control, Measurement, Electronics, Computing and Communications

ISSN: (Print) (Online) Journal homepage: www.tandfonline.com/journals/taut20

An eye bolt shape slotted microstrip patch antenna design utilizing a substrate-integrated waveguide for 5G systems

J. Merin Joshiba & D. Judson

To cite this article: J. Merin Joshiba & D. Judson (2023) An eye bolt shape slotted microstrip patch antenna design utilizing a substrate-integrated waveguide for 5G systems, Automatika, 64:4, 943-955, DOI: 10.1080/00051144.2023.2228065

To link to this article: https://doi.org/10.1080/00051144.2023.2228065

Published online: 25 Jul 2023.

AUTOMATIKA
2023, VOL. 64, NO. 4, 943–955
https://doi.org/10.1080/00051144.2023.2228065

An eye bolt shape slotted microstrip patch antenna design utilizing a substrate-integrated waveguide for 5G systems

J. Merin Joshiba[a] and D. Judson[b]

[a]Department of Electronics & Communication Engineering, DMI Engineering College, Nagercoil, India; [b]Department of Electronics & Communication Engineering, St. Xavier's Catholic College of Engineering, Nagercoil, India

ABSTRACT

Antenna design is usually done on FR4 substrates, since they have a dielectric constant of 4.4, and a loss tangent of 0.02. The proposed microstrip patch antenna operates at 28 GHz and incorporates substrate-integrated waveguides (SIW) in a 0.8 mm thick FR4 substrate into the design to increase bandwidth performance so that the 5G network can function reliably. In comparison with conventional patch antennas, substrate-integrated waveguides bear the advantage of being able to shift to a frequency of 29 GHz, therefore resulting in a more effective antenna. A slot of eyebolt shape has been added to the patch to increase antenna gain. The design was simulated with HFSS software, and it was able to attain a maximum bandwidth of 8 GHz (28%), a gain of 5.5 dB, and a minimal return loss of −38 dB. The VSWR of this antenna is 1.02, which indicates good impedance matching, and a high efficiency of 87% has been achieved as a result. This is a low-profile antenna that combines enhanced bandwidth with the ability to be mounted at the edge of a device, making it an ideal choice for the use of 5G technology to enable machine-to-machine communication.

ARTICLE HISTORY
Received 1 May 2023
Accepted 16 June 2023

KEYWORDS
Microstrip patch antenna; substrate-integrated waveguide; slot; bandwidth; 5G; HFSS

1. Introduction

A number of countries around the globe have implemented 5G because of its ability to offer ubiquitous connectivity and low latency [1]. A trail being blazed in many countries creates innovation for the twenty-first century [2]. This makes it possible to provide uninterrupted services such as online education that require a high data rate and high bandwidth [3]. In addition, it enables many other useful services such as the ability to connect appliances, access home security, carry out robotic farming remotely, monitor your health, track your shipping containers and logistics, and a number of other things. The provision of a large bandwidth is therefore necessary in order for all the services to be compatible with each other concurrently. For this reason, a new antenna needs to be designed in a compact size and to be equipped with special features [4],[5].

With increased bandwidth, this design works with 5G which is going to be introduced in many countries and which will revolutionize the way the world handles data communication [6]. For improving the bandwidth of an antenna, there are many performance enhancement techniques that can be applied, such as substrate material, shape of the antenna, slots in the antenna, metamaterial, substrate-integrated waveguide (SIW), etc., all of which can have an impact on the output performance. Shorting pins are one way of increasing gain by arranging an array of circularly polarized antennas [7],[8]. It is possible to communicate over milli-meter waves using an antenna array that consists of a multilayer PCB and an air-filled substrate [9], [10]. Furthermore, for the purpose of maintaining high isolation, different ports can be used [11]. In addition, an antenna which has a cavity-backed slot may also improve performance in applications requiring the capability to operate in the ISM band [12].

A key component of 5G systems is Multi-Input Multi-Output (MIMO) antennas that provide a good envelope correlation coefficient and ensure no loss in channel capacity over the spectrum. The substrate-integrated waveguide plays a significant role in enhancing bandwidth without compromising antenna performance which, in turn, facilitates the fabrication of printed circuit boards [13],[14]. Waveguides mounted on the substrate of the rectangular microstrip patch antenna increase bandwidth significantly, allowing for a variety of services to be carried out. Probably, when the future becomes more advanced, tri-band will be

CONTACT J Merin Joshiba merinjoshiba@gmail.com, merlinjoshibaj.dmi@outlook.com DMI Engineering College, Nagercoil, Tamil Nadu, India

able to meet the needs of these services as a starting point for multiband [15]. Hence, slow substrate-integrated waveguides with reduced antenna sizes have been developed to provide better performance for this application [16]. A defected ground structure was found to provide better return loss than an unflawed one, but at the price of a limited bandwidth [17]. Moreover, Air has been found to be a suitable substrate for fabricating antennas because it reduces fabrication costs and increases gain with less bandwidth [18]. SIW cavity-backed gap-coupled patch antennas are capable of addressing large bandwidth demands for future Internet of Things applications [19].

2. Exploration of a microstrip patch antenna design process

Located on the top of the substrate is the antenna, with the full ground plane at the bottom reducing the level of back radiation. Microstrip patch antennas are designed in accordance with

- Operating frequency, f_o.
- Height of the substrate, h_s.
- Relative Permittivity of the substrate, ϵ_r.

A common substrate used in these applications is FR4 because of its low cost and availability, with a ϵ_r of 4.4 and a loss tangent (tanδ) of 0.02. The antenna was developed for the 5G system using a substrate with a thickness of 0.8 mm, operating at 28 GHz.

a) The width W_p and length L_p of the patch are determined by

$$W = \frac{C}{2f_\circ\left(\frac{\sqrt{\varepsilon_r+1}}{2}\right)} \tag{1}$$

$$L_P = L_{eff} - 2\Delta L \tag{2}$$

$$L_{eff} = \frac{c}{2f_0\sqrt{\varepsilon_{eff}}} \tag{3}$$

$$\varepsilon_{eff} = \frac{\varepsilon_\gamma + 1}{2} + \frac{\varepsilon_\gamma - 1}{2}\left[1 + 12\frac{h_S}{w_P}\right]^{-1/2} \tag{4}$$

$$\Delta L = \left\{\frac{0.412(\varepsilon_{eff}+0.3)\left[\frac{w_P}{h_s}+0.264\right]}{(\varepsilon_{eff}+0.258)\left[\frac{w_P}{h_s}+0\cdot 8\right]}\right\} h_s \tag{5}$$

b) In order to determine the width W_s, W_g and length L_s, L_g of the substrate and the ground plane, respectively, the following equations can be used:

$$L_s = L_g = L_P + 6h_s \tag{6}$$

$$w_s = w_g = w_P + 6h_s \tag{7}$$

Table 1. Proposed antenna dimensions.

Parameter	Value (mm)
L_s	7
W_s	7
L_p	2.16
W_p	3.26
L_f	1.47
W_f	1.53
L_T	1.62
W_T	0.58
d	0.2
Mr	0.08
MR	0.175
SW	0.12
SL	0.7
W_1	0.1
W_2	0.27

c) As a design parameter, L_{fand} W_f of the microstrip feed line may be specified as follows:

$$L_f = \frac{90\cdot c}{\sqrt{\varepsilon_{eff}}\cdot\omega} \tag{8}$$

$$w_f = \begin{cases} \frac{2}{\pi}\left\{\begin{array}{c} B-1 \\ -\ln(2B-1) \\ +\frac{\varepsilon_\gamma-1}{2\varepsilon_\gamma} \\ \left[\ln(B-1)\right. \\ \left.+0.39-\frac{0.61}{\varepsilon_r}\right] \end{array}\right\} h_s, for\ \frac{w_P}{h_s} > 2 \\ \frac{8e^A}{e^{2A}-2}, \qquad for\ \frac{w_P}{h_s} < 2 \end{cases} \tag{9}$$

$$A = \frac{z_0}{60}\sqrt{\frac{\varepsilon_\gamma+1}{2}} + \left(\frac{\varepsilon_\gamma-1}{\varepsilon_r+1}\right)\left(0.23+\frac{0\cdot 11}{\varepsilon_\gamma}\right) \tag{10}$$

$$B = \frac{60\pi}{z_o\sqrt{\varepsilon_\gamma}} \tag{11}$$

d) The proposed system incorporates the inset feed in order to match the impedance between the antenna and the transmission line. A measurement of the inset cut's length Li and width Wi is given by

$$L_i = 4.65\times 10^{-22}\times\frac{Cf_\circ}{\sqrt{2\varepsilon_{eff}}} \tag{12}$$

$$w_i = \frac{L_P}{2\sqrt{\varepsilon_{eff}}} \tag{13}$$

e) The substrate-integrated waveguide design requires the following two conditions

$$\mathrm{d} < \frac{\lambda g}{5} \tag{14}$$

$$\mathrm{p} = 2\mathrm{d} \tag{15}$$

where d = diameter of metalized via hole

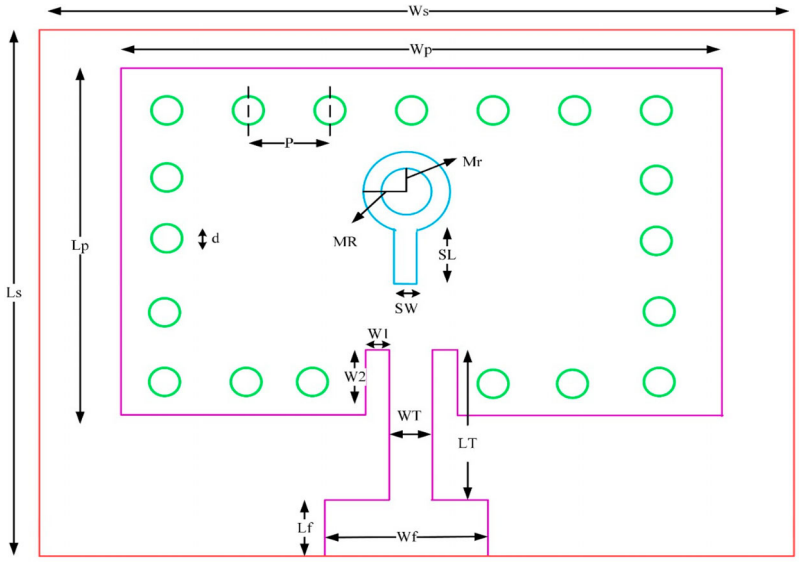

Figure 1. Configuration of proposed antenna

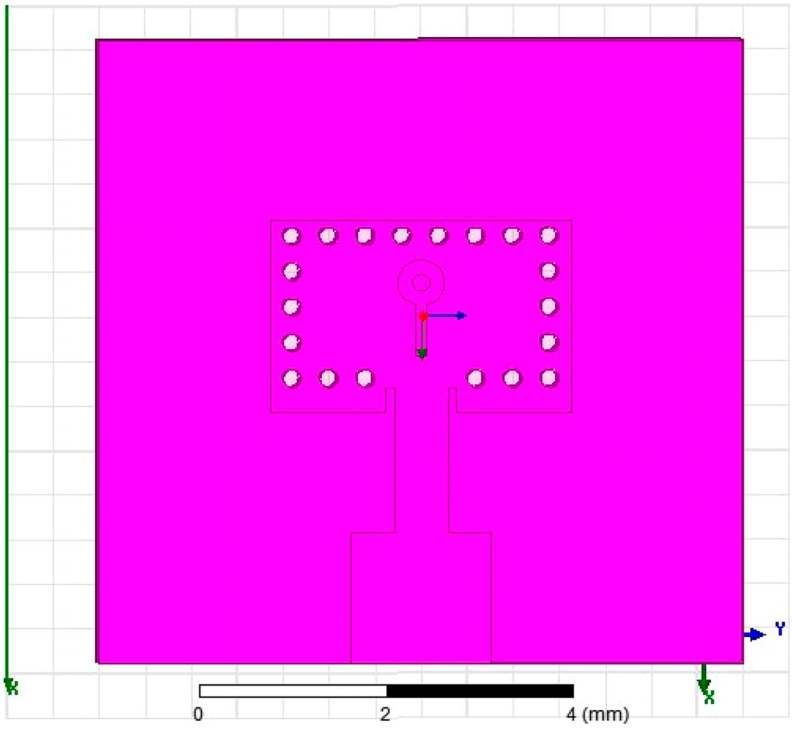

Figure 2. Top view of proposed design

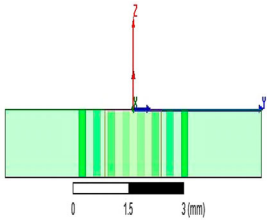

Figure 3. Side view of proposed design

p = pitch between adjacent via hole.

The design process of 28 GHz with different stages is explained in the following diagram.

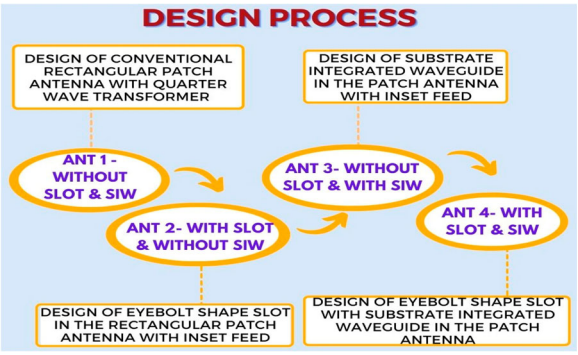

Figure 1 illustrates the proposed antenna design using HFSS software for use in 5G applications in the

28 GHz band. The design dimensions of this antenna are presented in Table 1.

As shown in Figures 2 and 3, the top view of the antenna is presented as well as the side view of the antenna.

3. Improved design and simulated results for the optimal patch antenna

This work involves the development and simulation of conventional rectangular microstrip patch antennas

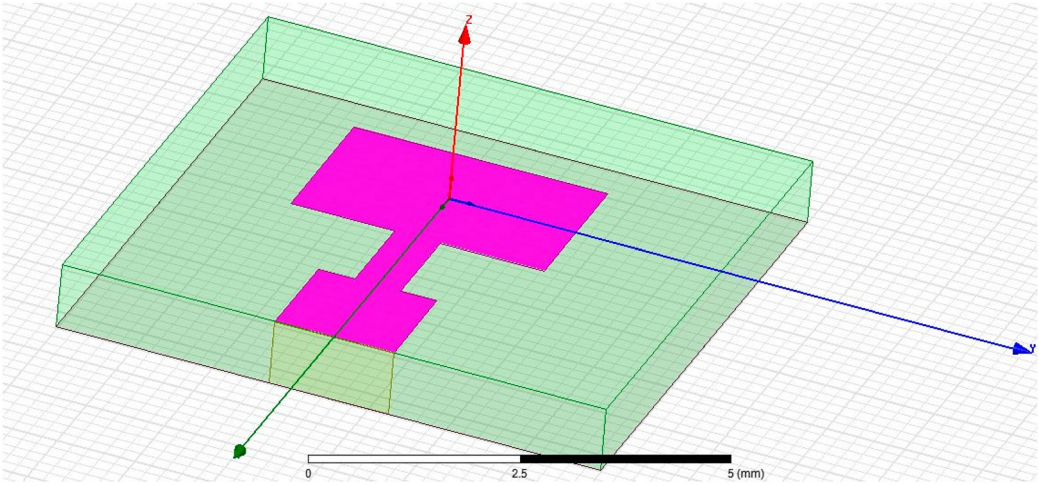

Figure 4. 3D Geometrical configuration of conventional Ant 1.

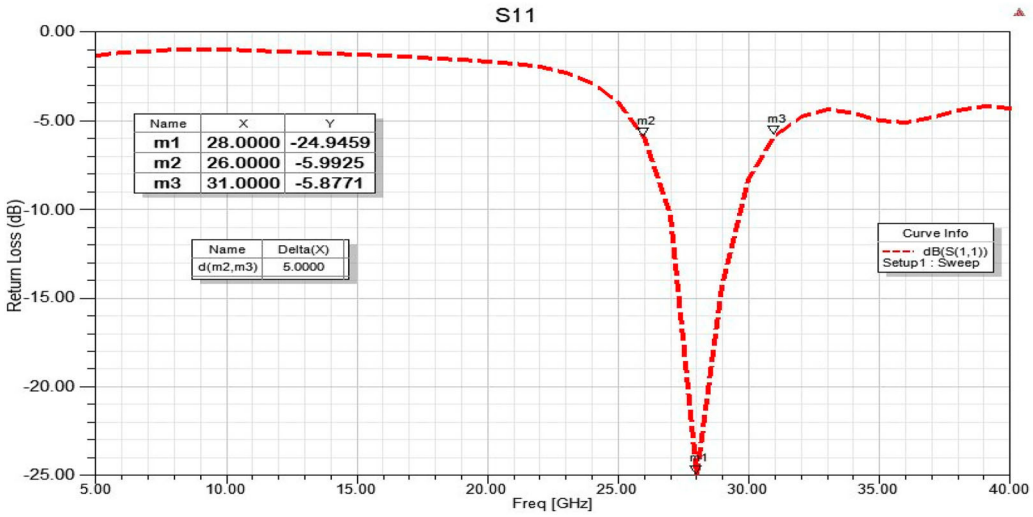

Figure 5. Loss characteristics of a conventional antenna configured for 5G based on its frequency.

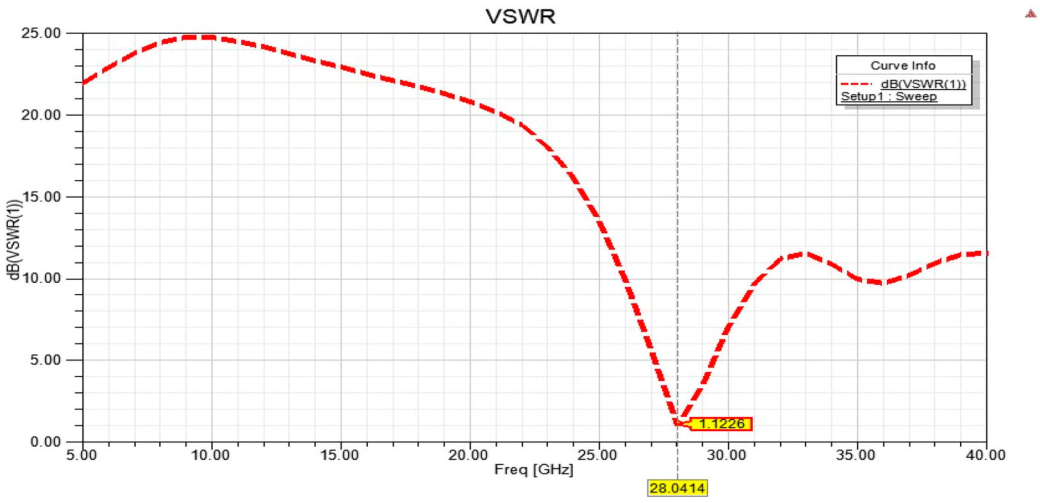

Figure 6. Diagram demonstrating the voltage standing wave ratio as a function of frequency for conventional antennas on a 5G network

(Ant1), a slotted patch antenna (Ant2), a substrate-integrated waveguide (SIW) patch antenna (Ant3), and a slotted SIW patch antenna (Ant4) using HFSS software. Antennas of the above design are fabricated using FR4 substrates, each of which has $\epsilon_r = 4.4$, tan $\delta = 0.02$ and thickness $(h_s) = 0.8$ mm. In the case of antenna without SIW cavity, the resonant frequency is 28 GHz, whereas in the case of an antenna with SIW cavity, it is 29 GHz. The bandwidth of the microstrip patch antenna is increased by incorporating substrate-integrated waveguides.

3.1. *Microstrip patch antenna without slot & SIW (Ant 1)*

A conventional rectangular microstrip patch antenna is shown in Figure 4 with a quarter-wave transformer.

Figure 5 illustrates the return loss of a conventional antenna that is suitable for 5G communication. The simulated return losses are less than −10 dB, which is about −24.9 dB at 28 GHz with 5Ghz bandwidth over the frequency bands 26Ghz to 31Ghz, which covers the required spectrum for 5G. This conventional antenna

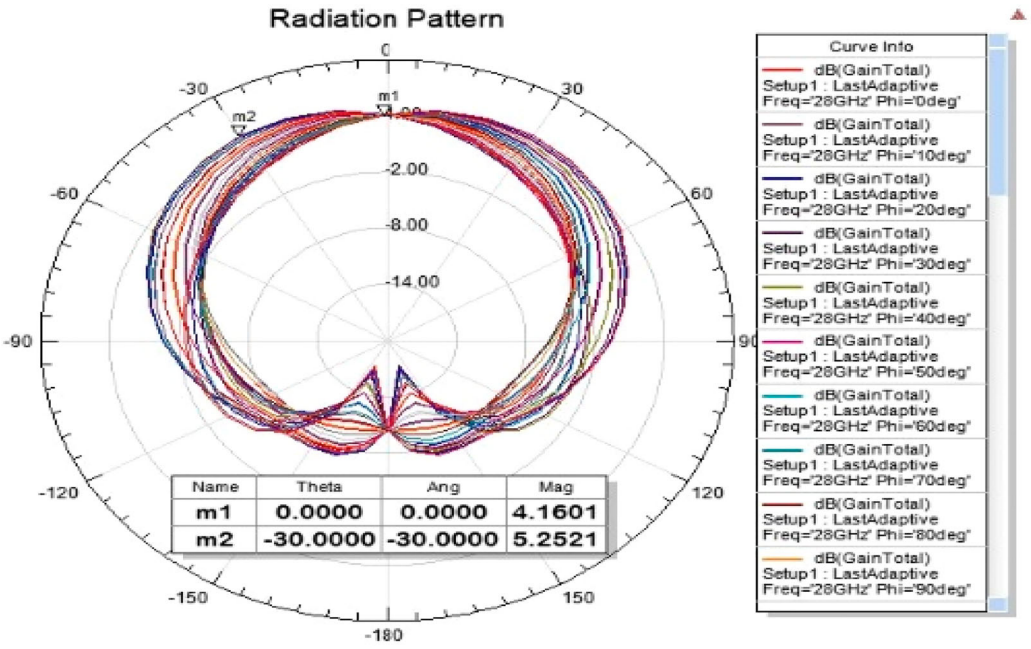

Figure 7. Total gain pattern of Ant 1 at 28Ghz along the xz and yz directions.

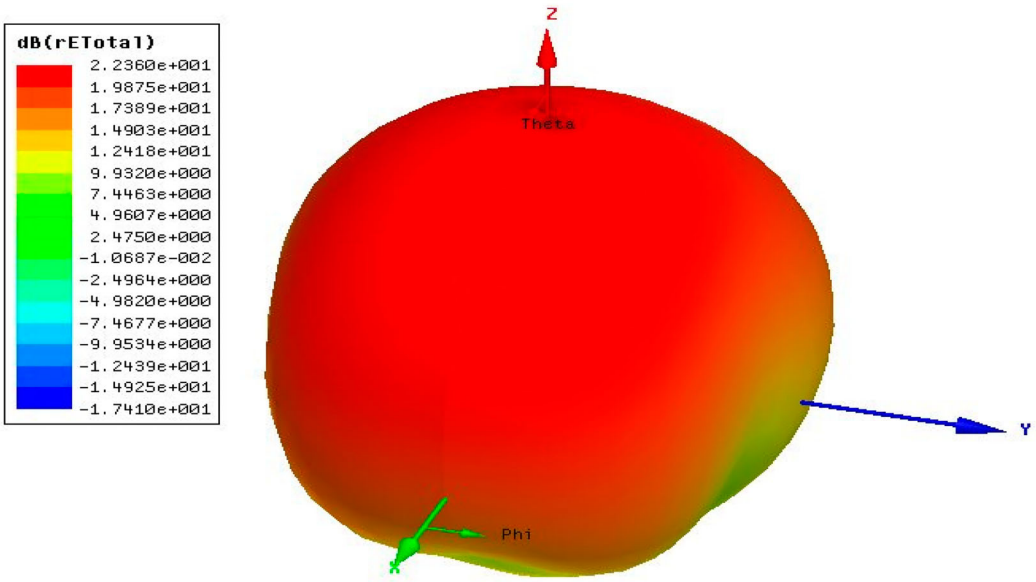

Figure 8. 3D radiation pattern of Ant 1 operating at 28Ghz

with a −24.9 dB return loss will match the impedance requirement. The VSWR value calculated using a resonance frequency of 28.00 GHz is 1.1226 as indicated in Figure 6. A plot of the total gain pattern is shown in Figure 7 for the angles of 0° to 90° in the planes. It achieves a peak gain of 5.25 dB at $\theta = -30^{\circ}$ and 4.16 dB at $\theta = 0^{\circ}$. Figure 8 shows a 3-dimensional representation of the radiation pattern for Ant 1 at 28 GHz in form of a 3D model.

3.2. Slotted microstrip patch antenna without SIW (Ant 2)

As shown in Figure 9, an eye bolt-shaped slotted microstrip patch antenna without SIW is represented in three dimensions with an inset feed for impedance matching.

In Figure 10, the Ant 2 performance with improved return loss is shown. It is bounded by −28.19 dB with 5.4Ghz bandwidth, which exceeds Ant1. Based on Figure 11, the VSWR value calculated at 28.00 GHz is 1.08. Using the same angle of 0° to 90° in the planes as shown in Figure 12, a plot of the total gain pattern is shown. During operation at $\theta = -30°$, it achieves a peak gain of 5.44 dB and at $\theta = 0°$, it achieves a peak gain of 4.29 dB. An illustration of the radiation pattern for Ant 2 at 28 GHz in the form of a 3D model is shown in Figure 13.

3.3. Microstrip patch antenna without slot & with SIW (Ant 3)

Ant 3 is intended to enhance the bandwidth of the network. With HFSS, the dimensions of the radiator, feedline, substrate, and slots in patch are adjusted as shown in Figure 14. The frequency changes to 29 GHz due to the substrate-integrated waveguides.

As illustrated in Figure 15, the Ant 3 has improved its performance as it has an improved return loss. As a result, it is constrained by −37.39 dB and has 8Ghz

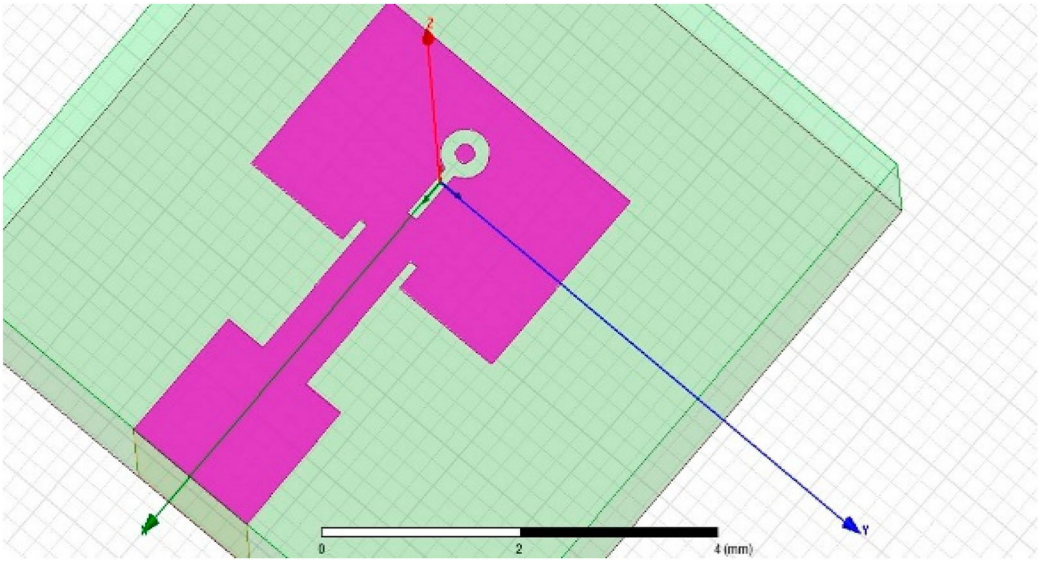

Figure 9. 3D Geometrical configuration of proposed Ant 2.

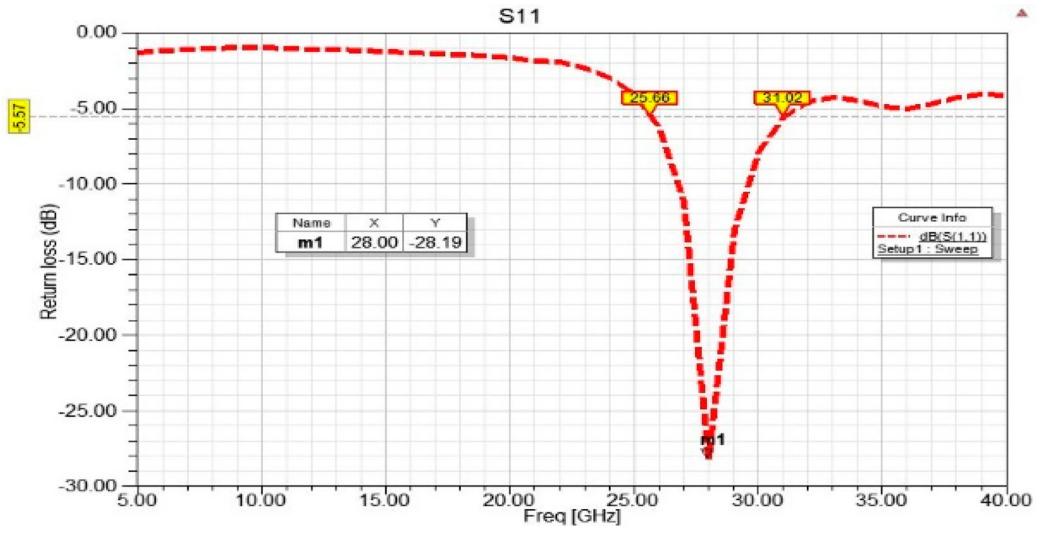

Figure 10. Loss characteristics of Ant 2 configured for 5G based on its frequency.

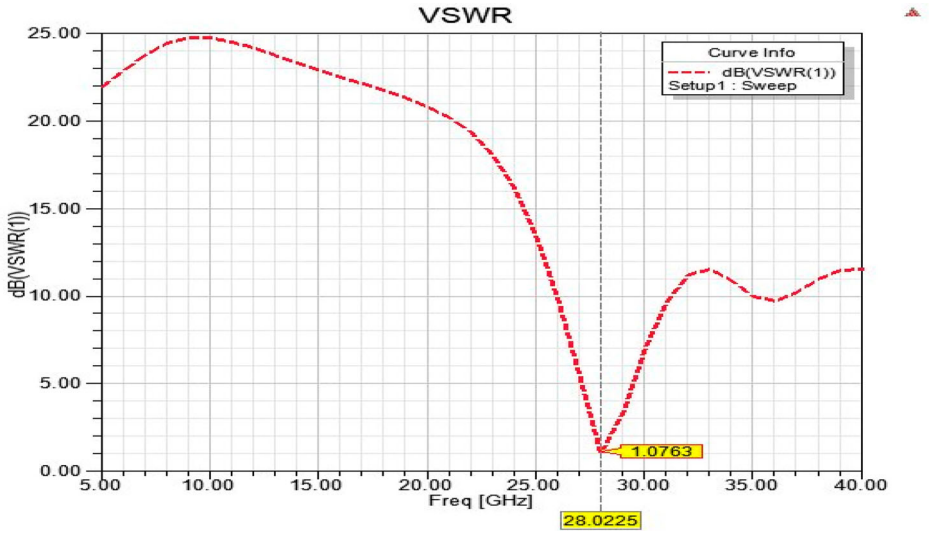

Figure 11. Diagram demonstrating the voltage standing wave ratio as a function of frequency for Ant 2 on a 5G network

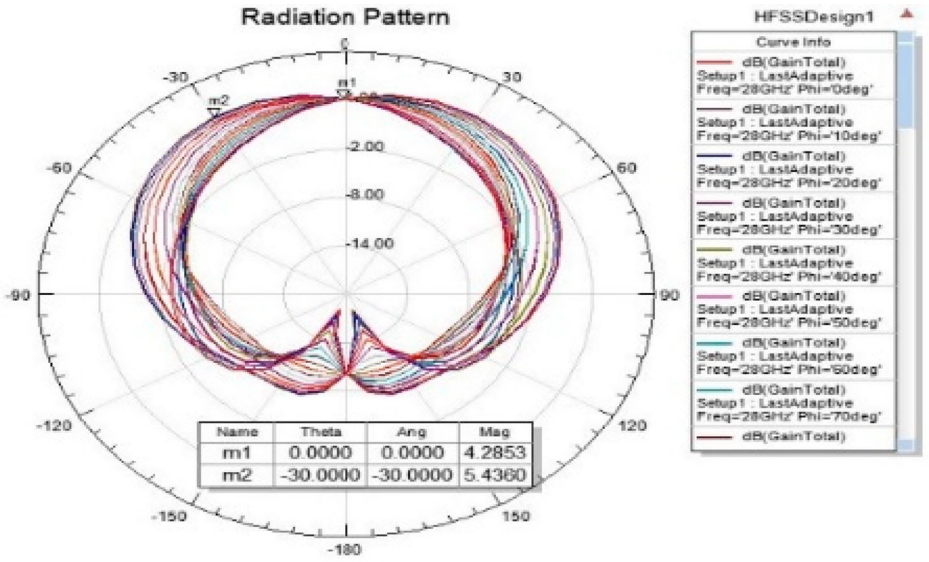

Figure 12. Total gain pattern of Ant 2 at 28Ghz along the xz and yz directions

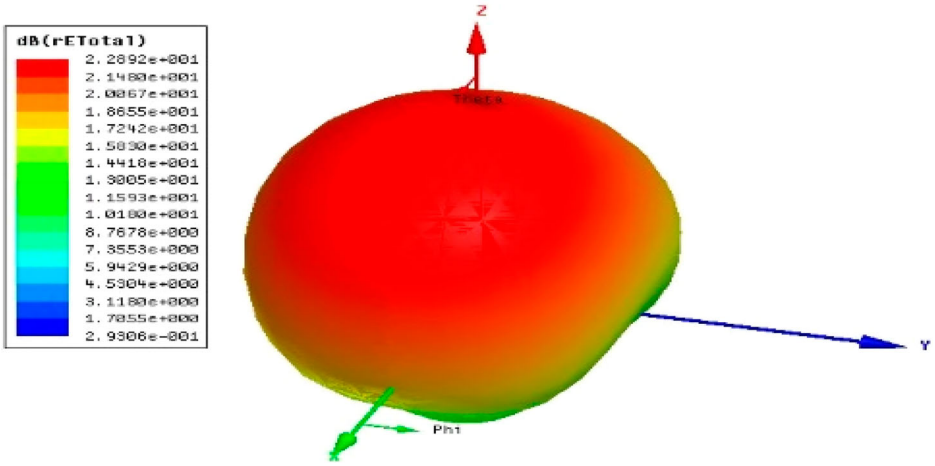

Figure 13. 3D radiation pattern of Ant 2 operating at 28Ghz

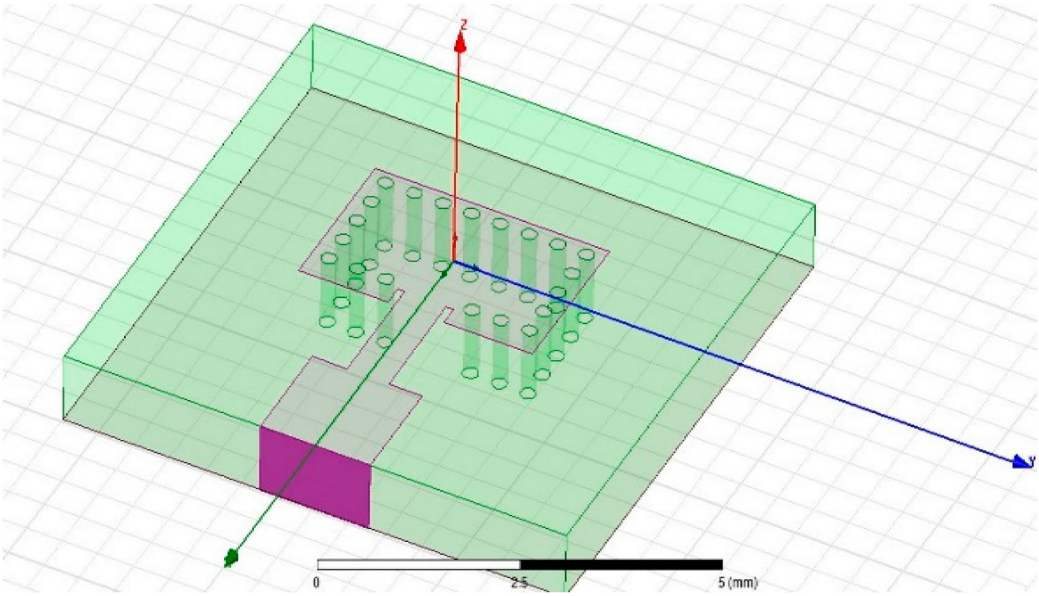

Figure 14. 3D Geometrical configuration of proposed Ant 3

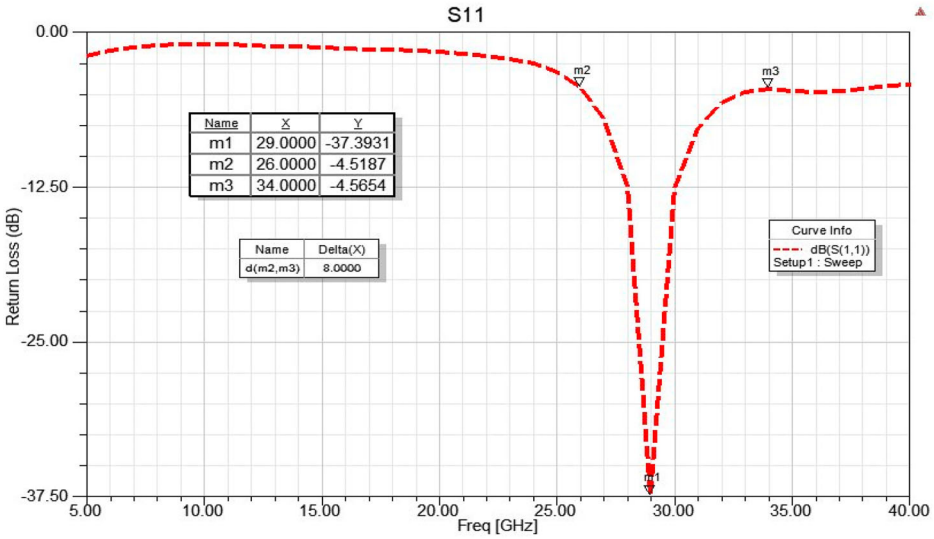

Figure 15. Loss characteristics of Ant 3 configured for 5G based on its frequency.

bandwidth, which is greater than that of Ant1 & 2. In accordance with Figure 16, the VSWR value calculated at 29.00 GHz is 1.0223. In Figure 17 where the planes are angled from $\phi = 0°$ to $\phi = 90°$, a plot of the total gain is illustrated. The maximum gain achieved at $\theta = -30°$ is 5.32 dB, and at $\theta = 0°$ it is 4.0 dB. The radiation pattern of Ant-3 at 29 GHz is shown in Figure 18 using a 3D visualization.

3.4. Slotted microstrip patch antenna with SIW (Ant 4)

Figure 19 illustrates the geometrical configuration of Ant 4 operating at 29 GHz with an eye-bolt shape slot in the substrate-integrated waveguide required for 5G communication.

It is noteworthy that Ant 4 had a return loss of −38 dB, which is higher than previous antennas. In terms of bandwidth, this antenna works at 8Ghz. Accordingly, Figure 20 shows the loss characteristics that can be attributed to Ant 4, which is suited for 5G. This antenna's VSWR value was found to be 1.0213 at 29.00 GHz, providing adequate impedance matching for 5G networks Figure 21. The gain pattern is shown in Figure 22, corresponding to $\phi = 0^{\circ}$ and $\phi = 90^{\circ}$. On the basis of the figure, it can be seen that the peak gain of Ant 4 is 5.5 dB at $\phi = 0^{\circ}$ and $\theta = -30^{\circ}$, and 4.00 dB at $\phi = 90^{\circ}$ and $\theta = 0^{\circ}$. A 3D simulation of the radiation pattern of Ant-4 operating at 29 GHz is shown in Figure 23 to illustrate the pattern.

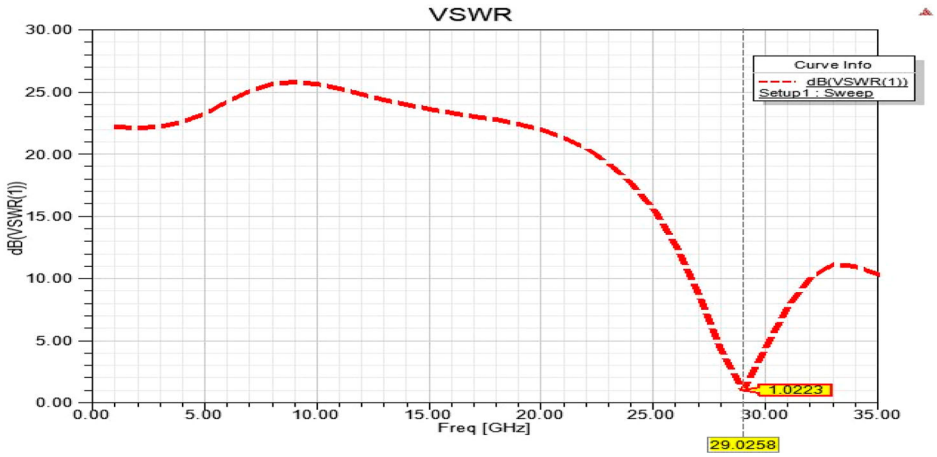

Figure 16. Diagram demonstrating the voltage standing wave ratio as a function of frequency for Ant 3 on a 5G network

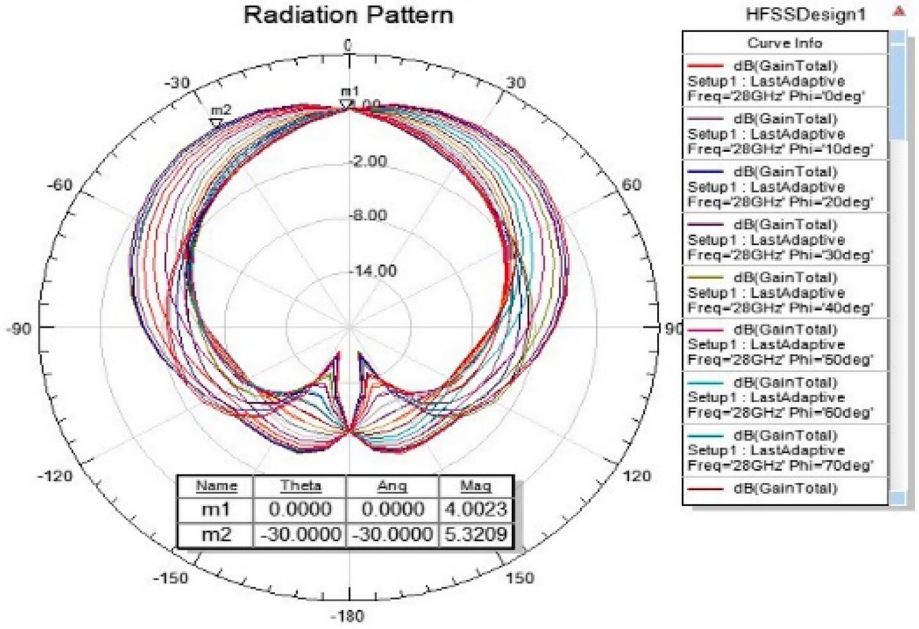

Figure 17. Total gain pattern of Ant 3 at 29Ghz along the xz and yz directions

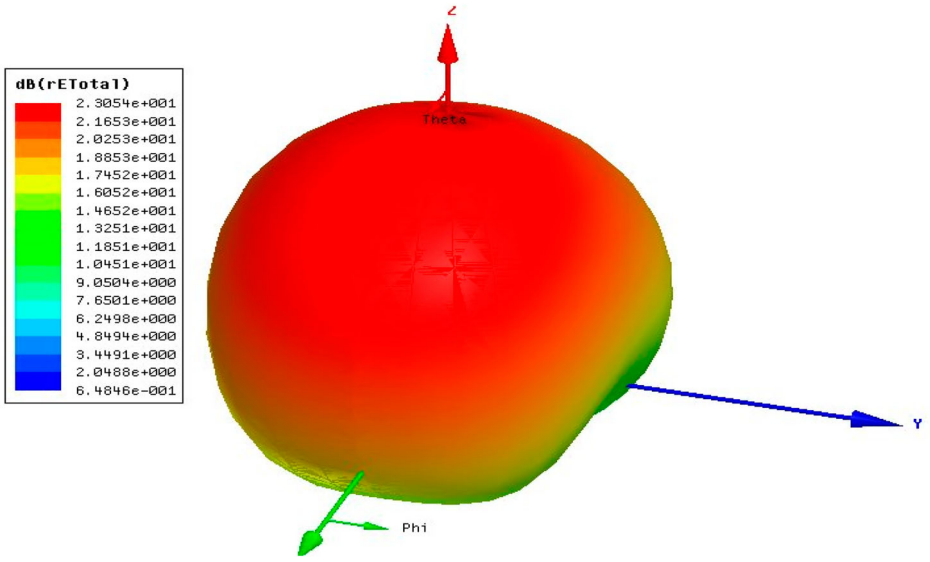

Figure 18. 3D radiation pattern of Ant 3 operating at 29Ghz

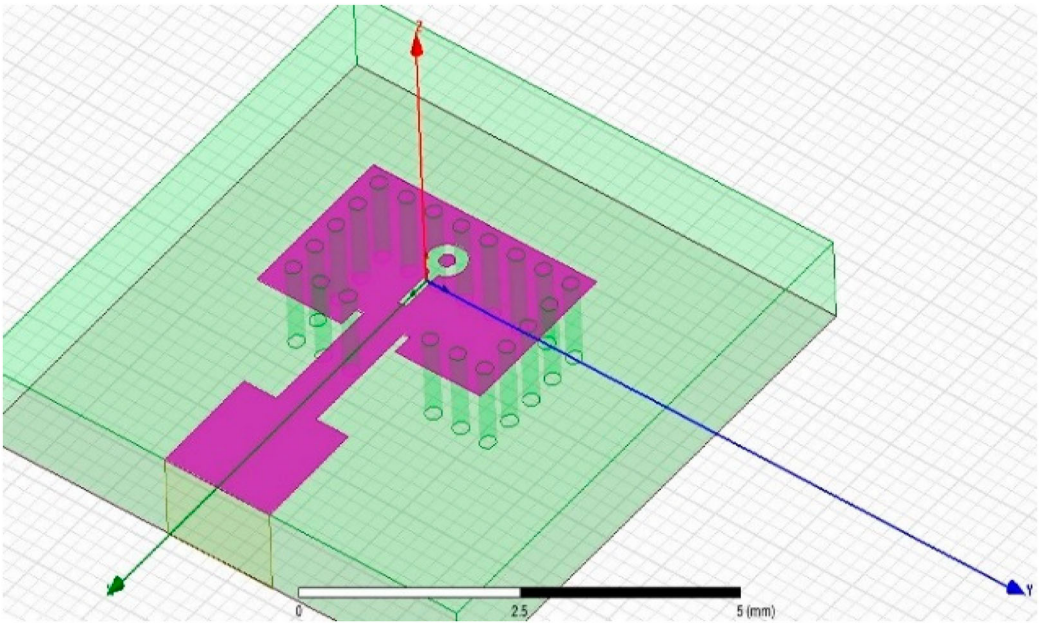

Figure 19. 3D Geometrical configuration of proposed Ant 4.

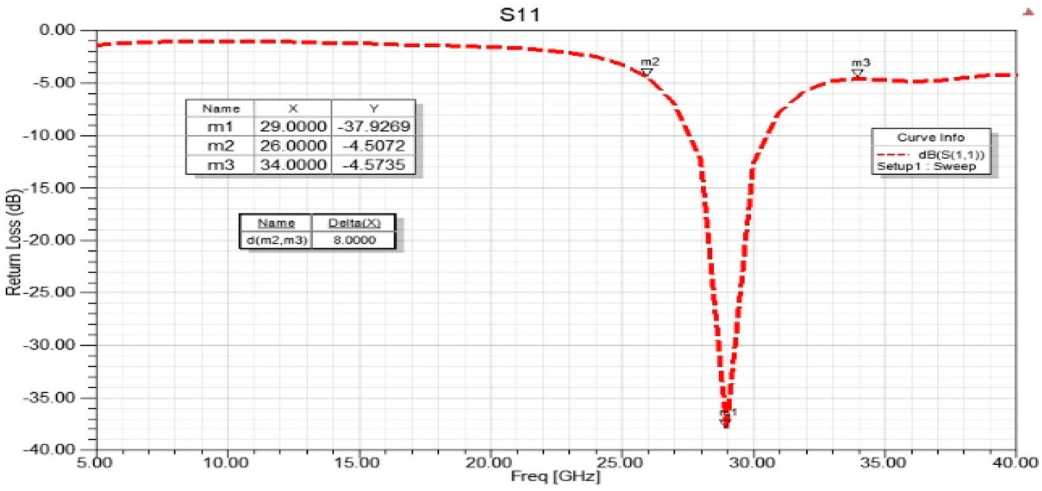

Figure 20. Loss characteristics of Ant 4 configured for 5G based on its frequency.

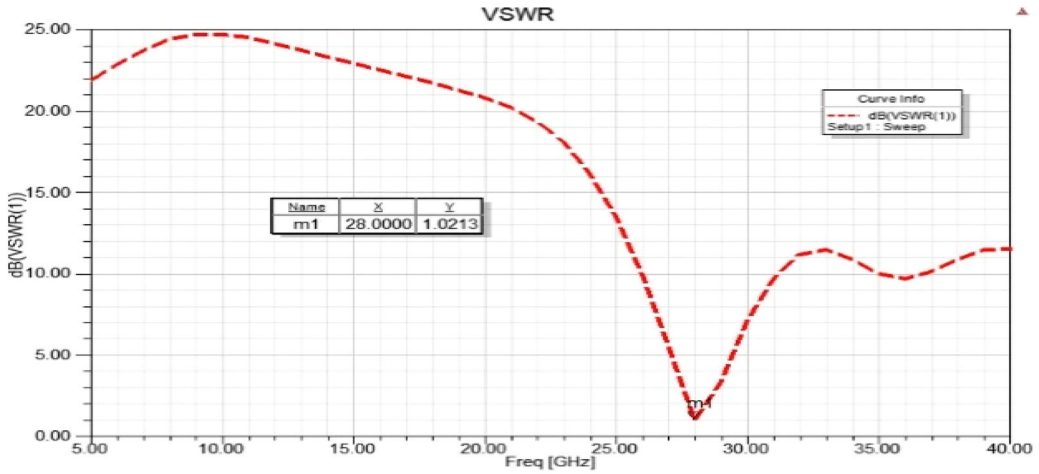

Figure 21. Diagram demonstrating the voltage standing wave ratio as a function of frequency for Ant 4 on a 5G network

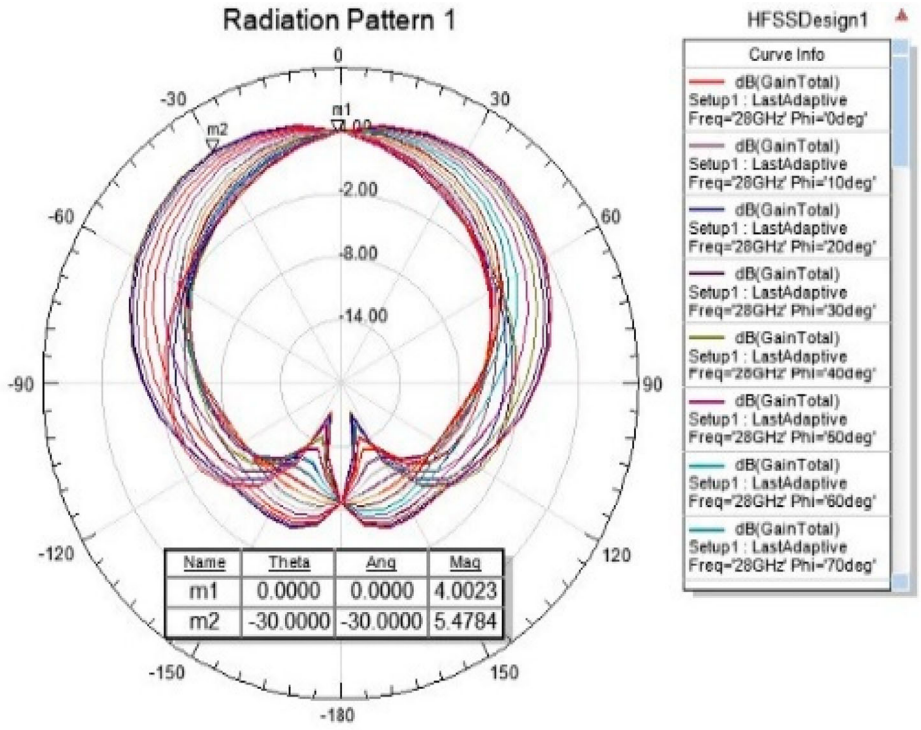

Figure 22. Total gain pattern of Ant 4 at 29Ghz along the xz and yz directions

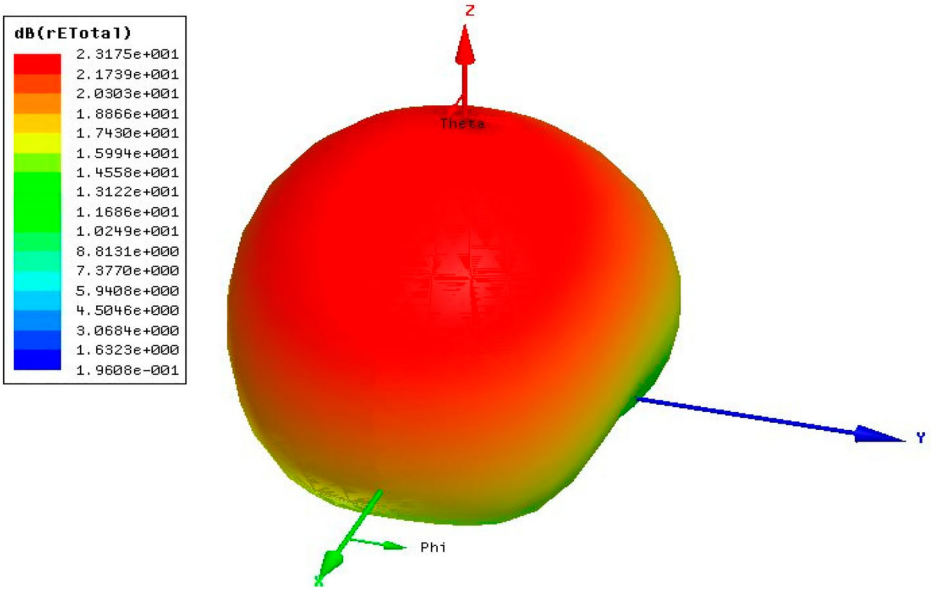

Figure 23. 3D radiation pattern of Ant 4 operating at 29Ghz

4. Comparison of the proposed antennas with other antennas

Presented in Table 2 are the various technical characteristics of proposed antennas such as Ant 2, Ant 3, and Ant 4, as compared to the conventional antenna, Ant 1.

A significant influence on antenna performance is the amount of return loss available to the antenna. Figure 24 illustrates the comparative graph of return loss by the proposed models. Table 3 gives the comparison of various size of the microstrip antennas. Of all the antennas mentioned in the table, the proposed antenna has increased to a maximum bandwidth of 8 GHz (28%) which provides more services in the 5G systems.

Table 2. Parameters and Evaluation of the results.

Parameters	Ant 1	Ant 2	Ant 3	Ant 4
Return loss (dB)	−24.9	−28.19	−37.39	−38
VSWR	1.12	1.08	1.0223	1.0213
Bandwidth (Ghz)	5	5.4	8	8
Gain (dB)	5.25	5.44	5.32	5.5
Radiated Power (dBm)	29.12	29.24	29.34	29.38
Efficiency (%)	81.66	83.95	85.9	86.7

5. Conclusion

In this paper, we propose the use of substrate-integrated waveguide antennas with an eyebolt shape slot to provide immense connectivity due to the necessity of

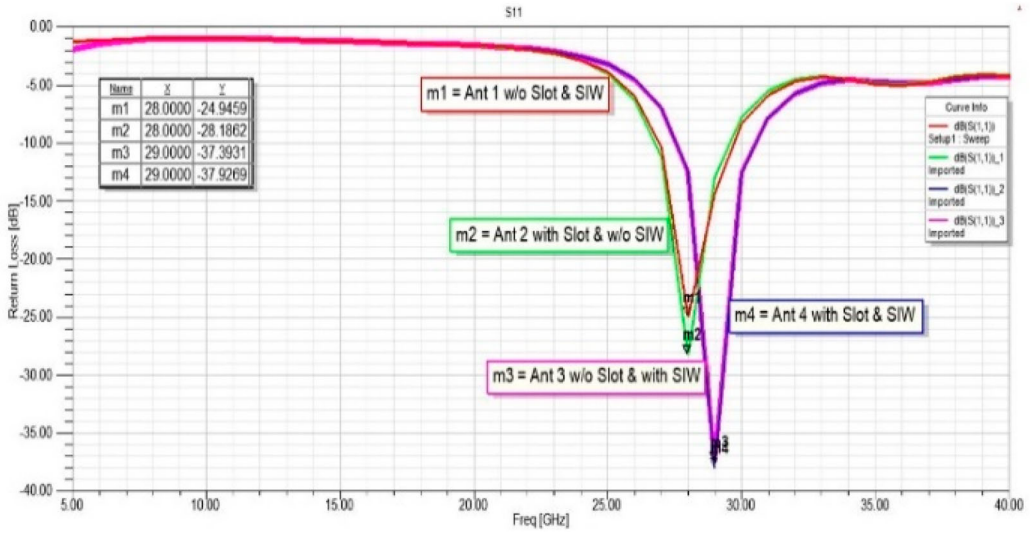

Figure 24. Comparative graph of the models proposed

Table 3. Analogy between the proposed antennas and other antennas.

Published Antenna	Size (mm)	Return loss (dB)	Band width (GHz)	Gain (dB)	Efficiency (%)
[20]	2.7 × 2.2	−30	1	8.4	84
[1]	30 × 15	−35	6.4	5.4	84
[2]	7 × 7	−39	2.48	6.3	86
[9]	.48 × 0.48	−13.25	7.15	7.4	85
[4]	6.2 × 8.4	−22.5	5.5	3.6	80
[10]	2.6 × 2.6	−30	2.4	6.2	-
[5]	5.3 × 4.5	−39	1.72	9.55	90
[17]	5 × 5	−56	1.38	7.6	98
Proposed Antenna	**7 × 7**	**−38**	**8**	**5.5**	**87**

5G systems, while providing low-latency at the same time. This new patch antenna can provide a much higher bandwidth than many traditional patch antennas due to the incorporation of substrate-integrated waveguides on the substrate, which raises the bandwidth of the proposed patch antenna to 28% at 28 GHz, which is still higher than many other conventional patch antennas. Using an eyebolt shape slot, the antenna is able to attain a gain of up to 5.5 dB, which translates to a higher gain for the user. The simulation is carried out using the HFSS tool and the efficiency of the system is estimated to be 87%, achieving return loss of −38 dB as well as VSWR of 1.02. It is therefore imperative to select the optimal performance technique for maximizing the bandwidth of this antenna, such as substrate-integrated waveguides.

Disclosure statement

No potential conflict of interest was reported by the authors.

References

[1] Hussain N, Awan WA, Ali W, et al. Compact wideband patch antenna and its MIMO configuration for 28 GHz applications. AEUE - Int J Electron Commun. 2021;132:153612, doi:10.1016/j.aeue.2021.153612

[2] kaeib AF, Shebani NM, Zarek AR. Design and analysis of a slotted microstrip antenna for 5G communication networks at 28 GHz. 19th international conference on sciences and techniques of automatic control & computer engineering (STA); March 24-26, 2019; Sousse, Tunisia, IEEE.

[3] Colaco J, Lohani R. Design and implementation of microstrip patch antenna for 5G applications. Fifth international conference on communication and electronics systems (ICCES 2020), IEEE xplore; July 11,2020, ISBN: 978-1-7281-5371-1.

[4] Przesmycki R, Bugaj M, Nowosielski L. "Broadband Microstrip Antenna for 5G Wireless Systems Operating at 28 GHz" Electronics 2021,10,1. https://www.mdpi.com/journal/electronics.

[5] Mohammed ASB, Kamal S, Fadzil Bin Ain M. Mathematical model on the effects of conductor thickness on the centre frequency at 28 GHz for the performance of microstrip patch antenna using air substrate for 5G application. Alexandria Eng J. December 2021;60(6):5265–5273. doi:10.1016/j.aej.2021.04.050

[6] Shamim SM, Dina US, Arafin N, et al. Design of efficient 37 GHz millimeter wave microstrip patch antenna for 5G mobile application. Plasmonics. 2021;16:1417–1425. doi:10.1007/s11468-021-01412-x

[7] Cheng Y, Dong Y. Wideband circularly polarized planar antenna array for 5G millimeter-wave applications. IEEE Trans Antennas Propag. October 2020;69(5):2615–2627. doi:10.1109/TAP.2020.3028213

[8] Fan C, Wu B, Wang Y-L, et al. High-gain SIW filtering antenna with low H-plane cross polarization and controllable radiation nulls. IEEE Trans Antennas Propag. August 2020;69(4):2336–2340. doi:10.1109/TAP.2020.3018595

[9] de Paula IL, Lemey S. Cost-effective high-performance air-filled SIW antenna array for the global 5G 26 and 28 GHz bands. IEEE Antennas Wirel Propag Lett. February 2021;20(2):194–198. doi:10.1109/LAWP.2020.3044114

[10] Yang Q, Gao S, Luo Q. Millimeter-wave dual-polarized differentially Fed 2-D multibeam patch antenna array. IEEE Trans Antennas Propag. October 2020;68(10):7007–7016. doi:10.1109/TAP.2020.2992896

[11] Kiran Kumar Dash S, Cheng QS, Barik RK, et al. A compact triple-fed high-isolation SIW based self-triplexing

antenna. IEEE Antennas Wirel Propag Lett. May 2020;19(5):766–770. doi:10.1109/LAWP.2020.2979488
[12] Chaturvedi D, Kumar A, Raghavan S. A nested SIW cavity-backing antenna for Wi-Fi/ISM band applications. IEEE Trans Antennas Propag. April 2019;67(4): 2775–2780. doi:10.1109/TAP.2019.2896670
[13] Hu H-T, Chan CH. Substrate-integrated-waveguide-fed wideband filtering antenna for millimeter-wave applications, IEEE Xplore, July 03,2021.
[14] Amer H, Abdulsattar MAK. Design of substrate integrated waveguide (SIW) antenna. Commun Appl Electron. June 2018;7(17):14–20. doi:10.5120/cae2018652774
[15] Abdelaziz A, Hamad EK. Design of a compact high gain microstrip patch antenna for tri-band 5 G wireless communication. Frequency. 2019;73(1–2):45–52. doi:10.1515/freq-2018-0058
[16] Ho AT, Pistono E, Corrao N, et al. Circular polarized square slot antenna based on slow-wave substrate integrated waveguide. IEEE Trans Antennas Propag. March 2021;69(3). doi:10.1109/TAP.2020.3030933
[17] Awan WA, Zaidi A, Baghdad A. Patch antenna with improved performance using DGS for 28 GHz applications. 2019 International conference on wireless Technologies, Embedded and Intelligent Systems (WITS); April 2019; Fez Morocco, IEEE. doi:10.1109/WITS.2019.8723828
[18] Kamal S, Mohammed ASB. A 28 GHz mmWave circular microstrip antenna with rectangular slots on Air-substrate. 2020 IEEE international RF and microwave conference (RFM) doi:10.1109/RFM50841.2020.9344772
[19] Cai S, Liu J, Long Y. Investigation of SIW cavity-backed slot and patch antennas with conical radiation patterns. IEEE Trans Antennas Propag. August 2020;68(8) doi:10.1109/TAP.2020.2990312
[20] Liu P, Zhu X-W, Zhang Y, et al. Patch antenna loaded with paired shorting pins and H-shaped slot for 28/38 GHz dual-band MIMO applications. IEEE Access. Feb 2020;8(11):23705–23712. doi:10.1109/ACCESS.2020.2964721